Journal of Global Positioning Systems (2013)
Vol.12, No.1 :73-82
DOI: 10.5081/jgps.12.1.73

Journal of Global Positioning Systems
2013
© CPGPS

Real-Time Assessment of GNSS Observation Noise with Single Receivers

Lei Wang, Yanming Feng, Charles Wang
Queensland University of Technology, Brisbane, Australia

Abstract

Stochastic modelling is critical in GNSS data processing. Currently, GNSS data processing commonly relies on the empirical stochastic model which may not reflect the actual data quality or noise characteristics. This paper examines the real-time GNSS observation noise estimation methods enabling to determine the observation variance from single receiver data stream. The methods involve three steps: forming linear combination, handling the ionosphere and ambiguity bias and variance estimation. Two distinguished ways are applied to overcome the ionosphere and ambiguity biases, known as the time differenced method and polynomial prediction method respectively. The real time variance estimation methods are compared with the zero-baseline and short-baseline methods. The proposed method only requires single receiver observation, thus applicable to both differenced and un-differenced data processing modes. However, the methods may be subject to the normal ionosphere conditions and low autocorrelation GNSS receivers. Experimental results also indicate the proposed method can result on more realistic parameter precision.

Keywords: stochastic model, variance estimation, GNSS observables, Multi-GNSS

---

1. Introduction

The mathematical model for GNSS positioning includes two aspects: the function model and the stochastic model. The function model describes the relationship between the observations and the parameters. The stochastic model describes the stochastic behaviours of the observations. An improved stochastic model not only improves the positioning precision, but also improves the quality control and ambiguity resolution. The stochastic model is typically described with the variance-covariance matrix, which includes precision, cross correlation and autocorrelation information.

Current stochastic model determination methods can be generally classified into four types:

- ***Empirical models:*** The constant model and elevation dependent model(Eueler & Goad, 1991; Jin & De Jong, 1996) belong to this category.. These empirical stochastic models describe the stochastic behaviours in a crude way and commonly in use due to its simplicity. The limitations of these methods are threefold: (1) they are not sensitive to the ionosphere condition and occasional events, such as ionosphere scintillation, solar storm et. al. (2) They cannot reflect the multipath error, as the multipath depends on the antenna design and observation environments. (3) the observations are not always dependent on the elevation angle (e.g. (Tiberius et al., 1999)). Furthermore, code noise depends on GNSS receiver internal algorithm. A typical sigma value of 0.3m for code noise level doesn't fit all receivers.
- ***External indicator:*** a typical indicator is C/N0 (Brunner et al., 1999; Hartinger & Brunner, 1999). The external indicator namely carrier to noise ratio (C/N0) or signal to noise ratio (SNR) is used to reflect the observation noise level. However, the SNR not only depends on the receiver, but also the antenna design.
- ***Estimation using posterior residuals:*** Stochastic model can be obtained by variance component estimation (VCE). The minimum quadratic unbiased estimation (MINQUE) method (Tiberius & Kenselaar, 2000; Wang et al., 2002) and the least-squares variance component estimation (LS-VCE) method (Amiri-Simkooei & Tiberius, 2007) have been used to estimate code variance as well as the correlations. However, these methods only are more suitable for processing the static GNSS data. Moreover, the uncertainty of the VCE solution may be unacceptable if the redundancy number is small.
- Estimation using observation combination: These methods eliminate all nuisance biases in GNSS observation by linear combination and reserve observation noise, includes the single differenced (SD) method (Bona, 2000; de Bakker et al., 2009; Li et al., 2008), the double differenced (DD) method (Borre & Tiberius, 2000; de Bakker et al., 2009) and the multi-differenced (MD) method (Kim & Langley, 2001). These methods are flexible and able

to reflect the actual noise variations. The problem is they need at least two receivers to overcome the ionosphere thus not applicable to zero differenced data processing.

The most common stochastic modelling approach is based on single differenced or double differenced code/phase observations using short-baseline or zero-baseline experiment (de Bakker et al., 2012; de Bakker et al., 2009; C. Tiberius et al., 2008).

Since the precise point positioning (PPP) mode becomes popular, the stochastic model estimation methods should also work with the zero differenced observations as well. However, the stochastic model estimation methods designed for the single-differenced or double differenced are no longer suitable. In addition, making use of the zero-differenced measurements enables to gain a better understanding of new GNSS signals in each direction.

In this study, a three-step procedure is introduced to estimate both code and carrier phase observation variance. The proposed method is independent from receiver motion status and positioning mode, thus flexible to apply to GNSS data processing.

2. Single-Receiver Variance Estimation

The GNSS signal consists of two parts: the signal and the noise. The signal part includes the geometry distance and various biases. The geometry distance contains the position states to be estimated and the biases contain the atmosphere effects and hardware delays. If all the biases are adequately considered, the observation noises determine the precision of the estimated parameters. In GNSS data processing, the nature of the observation noise is usually described by the variance-covariance matrix.

The major difference between various stochastic modelling methods lies in the different ways to separate the noise part from the signals. The original GNSS observation equation from each frequency can be given as:

$$\begin{aligned} P_i &= \rho + \delta_{orb} - c(\delta t_s - \delta t_r) + T + I_i + \varepsilon_{P,i} \\ \phi_i &= \rho + \delta_{orb} - c(\delta t_s - \delta t_r) + T - I_i - \lambda_i N_i + \varepsilon_{\phi,i} \end{aligned} \quad (1)$$

where P_i and ϕ_i are code observation and phase observation on i th frequency respectively; ρ is the geometry distance between the satellite transmitter and the receiver antenna; δ_{orb} is the orbit error; δt_s and δt_r are the satellite clock bias and the receiver clock bias. T and I_i are the troposphere delay and the ionosphere delay on i th frequency. λ_i and N_i are the wavelength and the unknown integer cycle number (ambiguity parameter) respectively. $\varepsilon_{P,i}$ and $\varepsilon_{\phi,i}$ are the signal noise (including the multipath error) for the code observation and the phase observation.

In the following subsections, the existing double-differenced model is briefly introduced and then the procedure of single receiver stochastic modelling method is discussed.

2.1 The double-difference method

The double-difference method is the most popular way to assess the stochastic model of the GNSS signals, e.g.(C. C. J. M. Tiberius et al., 2008). The double-differenced observation for short-baseline case can be expressed as:

$$\begin{aligned} \nabla\Delta P_i &= \nabla\Delta\rho + \nabla\Delta\varepsilon_{P,i} \\ \nabla\Delta\phi_i &= \nabla\Delta\rho - \lambda_i \nabla\Delta N_i + \nabla\Delta\varepsilon_{\phi,i} \end{aligned} \quad (2)$$

where $\nabla\Delta$ represents the double-difference operator. The satellite clock and receiver clock error terms are eliminated in double-differenced observation and the orbit error, ionosphere delay and troposphere delay are negligible in short-distance case. The observation noise measurement can be isolated once the baseline components $\nabla\Delta\rho$ are fixed. With correctly fixed ambiguity parameter, the observation of carrier phase can be isolated as well.

The double-differenced method requires two same type receivers and only suitable for double-difference positioning mode. The observations from different channels are inevitably correlated, and the original observation noise characteristics cannot be recovered precisely. The double-difference method is used as a reference method is the following discussion.

2.2 The single receiver method

The proposed single receiver noise assessment algorithm includes three steps: constructing linear combination, handling ionosphere and ambiguity and real time variance estimation. The ionosphere and ambiguity biases can be handled by either time-difference method or polynomial prediction method.

Construction of the linear combinations

As shown in Equation(1) the most of bias terms in the code and phase measurements are the same, thus the code noise can be isolated with the code-phase combination:

$$P_i - \phi_i \approx 2I_i + \lambda_i N_i + \varepsilon_{P,i} - \varepsilon_{\phi,i} \quad (3)$$

The remaining terms in the code-phase combination are doubled ionosphere delay, the ambiguity parameter, the signal noise. The carrier phase noise is only about 1/100 of the code noise, so the term $\varepsilon_{\phi,i}$ is ignorable. If the ionosphere and the ambiguity can be properly handled, the code noise $\varepsilon_{P,i}$ is separable.

Similarly, the carrier phase noise can be isolated by the Geometry-free (GF) linear-combination:

$$\phi_i - \phi_j = I_j - I_i - \lambda_i N_i - \lambda_j N_j + \varepsilon_{\phi,i} - \varepsilon_{\phi,j} \tag{4}$$

where the subscripts i and j stand for the frequencies. The carrier phase-based GF combination eliminates most bias terms in the observation and the remaining terms are the ionosphere delay, the ambiguity and the observation noise. It is noticed that the GF combination requires dual or multiple-frequency data, thus the combination is not available for single frequency users. If only considering the first order ionosphere effect, the differenced ionosphere delay can be expressed as:

$$I_j - I_i = \frac{f_j^2 - f_i^2}{f_i^2} I_i = \alpha_{i,j} I_i \tag{5}$$

where f_i and f_j are the i th and the j th frequency. $\alpha_{i,j}$ is the coefficient for short. Assuming $f_j < f_i$, $-1 < \alpha_{i,j} < 0$ holds for all GNSS systems.

Handling the ionosphere and the ambiguity biases

If the ambiguity parameters remain constant (no spikes and cycle slip) and the ionosphere varies smoothly, the remaining systematic biases can be handled by the time-difference method or the polynomial predication method.

The time-differenced observations take the difference between two consecutive epochs and can be expressed as:

$$\begin{aligned} \Delta_{P,i,m} &= (P_{i,m} - \phi_{i,m}) - (P_{i,m-1} - \phi_{i,m-1}) = 2\Delta I_{i,\Delta t} + \varepsilon_{P,i,m} - \varepsilon_{P,i,m-1} \\ \Delta_{\phi,m} &= (\phi_{i,m} - \phi_{j,m}) - (\phi_{i,m-1} - \phi_{j,m-1}) = 2\alpha_{i,j} \Delta I_{i,\Delta t} + \varepsilon_{\phi,m} - \varepsilon_{\phi,m-1} \end{aligned} \tag{6}$$

where $\Delta_{P,i,m}$ and $\Delta_{\phi,m}$ denote the time differenced observations on m th epoch for i th frequency; The subscript Δt stands for the time interval between $m-1$ th epoch and m th epoch. $\Delta I_{i,\Delta t}$ denotes the ionosphere delay variation on i th frequency over the period of Δt.

It is noticed that the ionosphere cannot be completely eliminated by time difference. The expectation and the variance of the time-differenced can be given as:

$$\begin{aligned} &E(\Delta_{P,i,m}) = 2\Delta I_{i,\Delta t}, E(\Delta_{\phi,i,m}) = 2\alpha_{i,j} \Delta I_{i,\Delta t} \\ &D(\Delta_{P,i,m}) = 4\sigma^2_{\Delta I_{i,m}} + 4(1-\rho_{\Delta t})\sigma^2_{\varepsilon_{P,i,m}} \\ &D(\Delta_{\phi,i,m}) = 4\alpha^2_{i,j}\sigma^2_{\Delta I_{i,m}} + 16(1-\rho_{\Delta t})\sigma^2_{\varepsilon_{\phi,i,m}} \end{aligned} \tag{7}$$

where $E(\cdot)$ and $D(\cdot)$ are mathematical expectation and dispersion operator. $\sigma^2_{\Delta I_{i,m}}$, $\sigma^2_{\varepsilon_{P,i,m}}$ and $\sigma^2_{\varepsilon_{\phi,i,m}}$ are the variance of the ΔI_i, $\varepsilon_{P,i}$ and $\varepsilon_{\phi,i}$ on m th epoch respectively. $\rho_{\Delta t}$ is the autocorrelation between two epochs. It is assumed the variances of $\varepsilon_{\phi,i}$ and $\varepsilon_{\phi,j}$ are the same. The code and phase variance remain unchange between two consecutive epochs.

Equation (7) illustrates that the time-differenced observations $\Delta_{P,i,m}$ and $\Delta_{\phi,m}$ are not zero means. The ionospheric delay increment ΔI_i still remains in the differenced observations. The variances of $\Delta_{P,i,m}$ and $\Delta_{\phi,m}$ are also affected by the autocorrelation. The magnitude of ΔI_i and the impact of autocorrelation are related to the interval Δt. The details of the ionosphere change and autocorrelation are discussed in next section.

The biases in equations (3) and (4) can be described by a low order polynomial, which is given as:

$$L_m = \Sigma_{j=0}^{k-1} e_j t_m^j \tag{8}$$

where L_m can be the code-phase GF combination $P_i - \phi_i$ or the carrier phase-based GF combination $\phi_i - \phi_j$ on the m th epoch. t_m is the time index of the m th epoch with respect to a reference time epoch; $e_1, \cdots, e_{k-1}$ are the coefficients of the polynomial. k is the polynomial order. The coefficients $e_1, \cdots, e_{k-1}$ can be estimated with the standard least-squares procedure. The fitted model is used to predict the upcoming epochs. The observation noise can be isolated with:

$$\begin{aligned} \Delta_{P,i,m+1} &= (P_{i,m+1} - \phi_{i,m+1}) - \Sigma_{j=0}^{k-1} \hat{e}_j t_{m+1}^j = \varepsilon_{P,i,m+1} \\ \Delta_{\phi,m+1} &= (\phi_{i,m+1} - \phi_{j,m+1}) - \Sigma_{j=0}^{k-1} \hat{e}_j t_{m+1}^j = 2\varepsilon_{\phi,m+1} \end{aligned} \tag{9}$$

where the subscript $m+1$ means the $m+1$ th epoch. $\hat{e}_j$ are the coefficients estimated with historical observations.

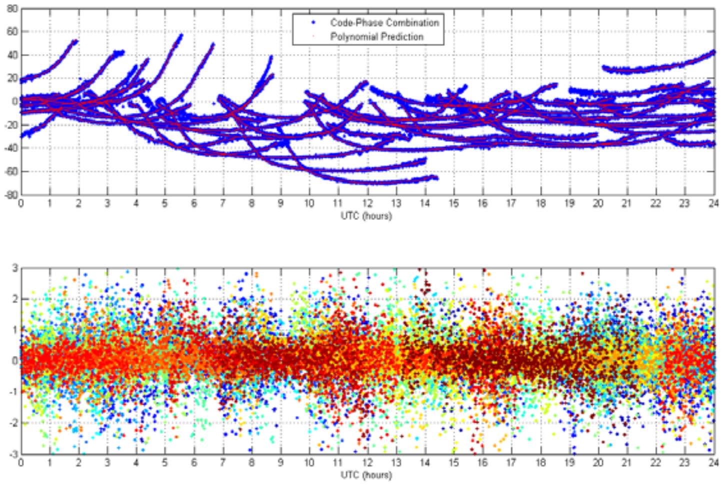

Figure 1: Illustration of polynomial prediction effects and the residuals. The upper panel presents the code-phase combination (blue dots) and the polynomial prediction value (red dots). The lower panel illustrates the difference between the prediction and the observation.

The term $\Sigma_{j=0}^{k-1}\hat{e}_j t_{m+1}^j$ is the prediction of the lumped ambiguity and ionosphere term from previous epochs. How the polynomial fit the ionosphere changes over hours of data arcs is presented in Figure 1. The upper panel presents the code-phase combination (blue dots) and the polynomial prediction values (red dots) for all satellite passes over 24 hours. The lower panel shows the prediction residuals. Normally, the ionosphere varies smoothly and the low order polynomial can describe its variation well. Therefore, the residuals can be used to evaluate the observation noises.

Real-time variance estimation

In order to meet real-time data processing requirement, the observation variance has to be estimated on epoch basis. The linear combination constructed by the time-difference method and the polynomial prediction methods are considered (or approximately considered) as zero mean, their expectation and variance can be estimated by a moving-window average method, which can be given as:

$$E_{\Delta_{i,m}} = \frac{\sum_{k=m-l+1}^{m-1} \beta_k E_{\Delta_{i,m-1}} + \Delta_{i,m}}{\sum_{k=m-l+1}^{m} \beta_k l}$$
$$\sigma^2_{\Delta_{i,m}} = \frac{\sum_{k=m-l+1}^{m-1} \beta_k^2 (\Delta_{i,k} - E_{\Delta_{i,k}})^2 + (\Delta_{i,m} - E_{\Delta_{i,m}})^2}{\sum_{k=m-l+1}^{m} \beta_k l} \quad (10)$$

where $\Delta_{i,m}$ stands for $\Delta_{P,i,m}$ or $\Delta_{\phi,i,m}$ constructed with time differenced method or polynomial prediction method. l is the window length. $E_{\Delta_{i,m}}$ and $\sigma^2_{\Delta_{i,m}}$ are the expectation and variance of code and phase measurements on i th frequency and m th epoch respectively. The term β_k is so-called decay factor, which gives different weight to different epoch data. Generally, the old data have a smaller contribution to the estimates, so it deserves smaller decay factor. In equation(10), the decay factor of current epoch is set as 1, so the decay factors for the historical information should be in the interval [0,1]. The simplest case is the $\beta_k = 1$, all information is equal-weighted in this case. The window length depends on the sample rate and ionosphere activity.

The final step is to recover the original code variance. If the ionosphere variation and autocorrelation are ignored, the original code and phase observation noise for time difference method can be calculated with:

$$\sigma^2_{P,i,m} = \frac{1}{4}\sigma^2_{\Delta_{P,i,m}}$$
$$\sigma^2_{\phi,m} = \frac{1}{16}\sigma^2_{\Delta_{\phi,m}} \quad (11)$$

Similarly, the original code and phase observation noise for the polynomial prediction method can be calculated with:

$$\sigma^2_{P,i,m} = \sigma^2_{\Delta_{P,i,m}}$$
$$\sigma^2_{\phi,m} = \frac{1}{4}\sigma^2_{\Delta_{\phi,m}} \quad (12)$$

where $\sigma^2_{P,i,m}$ and $\sigma^2_{\phi,m}$ are the recovered original code and phase observation of m th epoch.

3. Limitations of the Single Receiver Variance Estimation Method

The methods discussed in the previous section are simple, but their performance suffers from a number of factors. Two major factors are the ionosphere variation and the autocorrelation, which were ignored in previous discussion. These factors may affect the performance of the single receiver variance estimation method in real data processing. Thus, it is important to understand their impacts before applying the method.

3.1 The ionosphere variation

In the time difference method, the ionosphere delay is only partially eliminated. The characteristics of the ionosphere variation $\Delta I_{i,\Delta t}$ have to be analysed.

The precise ionosphere variation can be isolated with dual frequency carrier phase observations, given as:

$$\Delta I_{i,\Delta t} \approx \frac{(\phi_{i,m} - \phi_{j,m}) - (\phi_{i,m-1} - \phi_{j,m-1})}{2\alpha_{i,j}} \qquad (13)$$

Assuming there are no cycle slips and loss-of-lock, the ambiguity parameters can be completely eliminated by the time difference procedure. The observation noise of carrier phase measurements is only a few millimetres, thus can be ignored. The ionosphere delay variation over Δt can be estimated with the equation(13).

In order to investigate the ionosphere variation, the IGS station COCO is selected as it located near the geomagnetic equator. According to the solar activity cycle, three days GPS observations with high solar activity on 1st, January, 2001, medium solar activity on 1st, January, 2004 and a low solar activity on 1st, January, 2009 are analysed. The ionosphere variations are presented in Figure 2. The figure shows the ionosphere variation rate largely depends on the solar activity. In high solar activity year, the solar variation can researches up to 5mm/s while in the low solar activity year, the solar variation is typically less than 1mm/s. The ionosphere variation is more significant in the daytime than in the night for all three cases. Furthermore, the ionosphere delay changes rapidly at the low elevation angle cases.

The large ionosphere variation can impact the expectation $E(\Delta_{P,i,m})$ and the variance of the time-differenced observation $D(\Delta_{P,i,m})$ .In this case, the expectation $E(\Delta_{P,i,m})$ cannot be treated as zero. The ionosphere residuals will be assimilated into $D(\Delta_{P,i,m})$ automatically. As a result, the estimated observation noise level would be larger than the real one. Meanwhile, it is noticed the ionosphere impact on the carrier phase GF combination is smaller than the code-phase combination since the coefficient $\alpha_{i,j}$ is smaller than 1. $\alpha_{i,j}$ is approximately equal to -0.393 and -0.340 for GPS L1/L2 combination and Beidou B1/B2 combination respectively. Thus the carrier phase GF combination is able to resist larger ionosphere variation than the code-phase combination.

The magnitude of ionosphere residuals depends on the ionosphere variation rate and the sampling interval. For

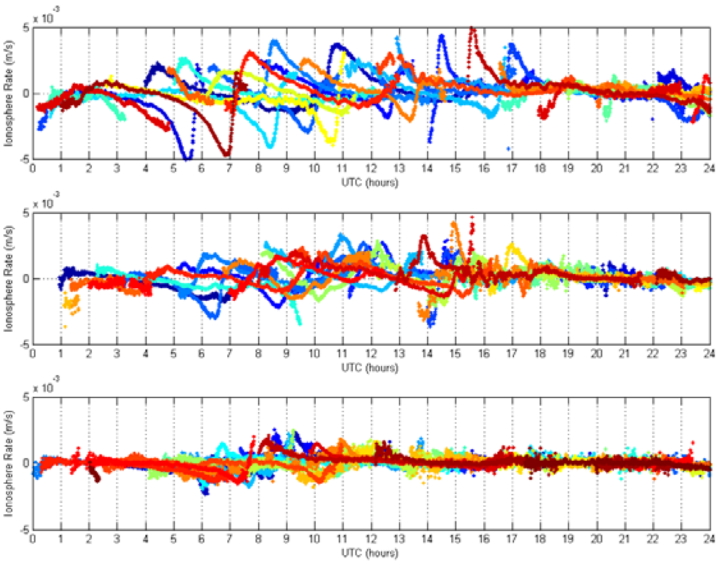

Figure 2: Ionosphere variation rate on GPS L1 signal. The figure shows high solar activity case (upper panel), medium solar activity case (middle panel) and low solar activity case (lower panel) respectively.

high rate GNSS data (e.g. 1Hz), the ionosphere residuals are always ignorable, while in the low sampling rate case (e.g. 30s interval), the ionosphere residuals can be too large. In this case, the observation noise can be estimated with both time differenced method and the polynomial fitting method. The polynomial fitting procedure can remove the remaining ionosphere residuals in the time-differenced observations.

3.2 The autocorrelation

The autocorrelation is another factor impacting the performance of the time difference methods. The autocorrelation characteristic depends on the internal algorithm of the GNSS receiver. The autocorrelation is defined as (e.g. Bona, 2000):

$$\rho(t,t+\tau)=\frac{E((X_t-\mu_t)(X_{t+\tau}-\mu_{t+\tau}))}{\sigma_t\sigma_{t+\tau}} \qquad (14)$$

where τ is known as time lag. μ_t and σ_t are the mathematical expectation and variance of the time series on time t respectively.

As shown in the equation(7), the autocorrelation leads to the estimated observation noise over-optimistic, especially for high rate data. The impact of autocorrelation is demonstrated with the following experiment. About 1 hour high rate (1Hz) data is collected with Novatel OEM 6T receivers and Trimble Net R9 receivers respectively. The autocorrelation is estimated with zero-baseline method, the estimated autocorrelation is presented in Figure 4. The figure shows the observation from Novatel OEM 6T receiver has a strong autocorrelation in a short time period, while the autocorrelation in Trimble Net R9 receiver is relatively low.

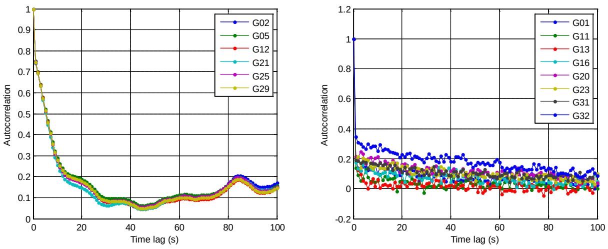

Figure 3: Illustration of the autocorrelation estimated with the zero baseline data. The data sets are collected with the Novatel OEM 6T receiver (left panel) and Trimble Net R9 receiver (right panel) respectively.

With the same observation data set, the code variance estimated with the time difference method. The estimated code standard deviation versus time lag is presented in Figure 4. The figure shows that there is little dependency of the estimated code variance on the time lags using the Trimble receiver, while the code variance increases dramatically with the time lag increases with the Novatel receiver. In this case, the observation variance estimation with the time-difference method is not generally applicable. Fortunately, the presence of autocorrelation is detectable with single receiver. Checking the autocorrelation characteristic of a receiver before data processing is necessary, as it gives some insight to the receiver's stochastic model. In the high autocorrelation case, the zero-baseline method or short baseline method provides more realistic estimation for variance estimation.

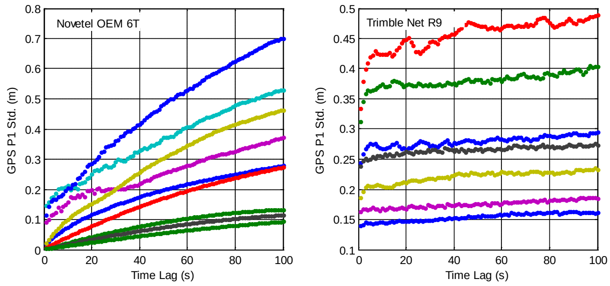

Figure 4: Illustration of the autocorrelation impact on estimated code variance with the time-difference method. The data sets are observed with Novatel OEM 6T receiver (left panel) and Trimble Net R9 receiver (right panel) respectively.

The ionosphere and the autocorrelation are the dominate issues affecting the performance, while the methods still may affected by other factors (e.g. the cross correlation can impact the carrier phase variance estimation since it requires observations from different channels). The cycle slip detection in carrier phase observation data processing and the outlier detection issues are also important in real time variance estimation.

4. Validation of the Single Receiver Variance Estimation Methods

Two experiments are designed to validate the performance of the single receiver variance estimation methods. The observation variance estimated with single receiver is compared with the double differenced method independently.

4.1 Case 1: High sampling rate data case

The comparison is made between zero-baseline method and time-difference method with the data set at 1 second interval data. GPS/BDS observations are collected with a Trimble Net R9 receiver. High rate observation can mitigate the ionosphere residuals and multipath error in the time-differenced code-phase combination. The observation standard deviations (STD) are estimated with three methods: the time-difference d method, the polynomial prediction method and the zero baseline method. The overall STD values of each GPS satellite are presented in Figure 5. The figure shows that the code

STD estimated from the zero baseline method is the smallest since the method can eliminate all error sources (including multipath) efficiently. The code STD estimated from the time-difference method is smaller than that of the polynomial prediction method. The overall STD values from the time-difference method and the polynomial method are around 0.3m, which is close to the empirical model. The STD values of carrier phase measurements estimated from the three methods are about 1 to 1.5 mm, while the polynomial prediction method is slightly larger STD than the other two methods. This is because the impact of the multipath error on the carrier phase is much smaller than the code measurement (Langley, 1996).

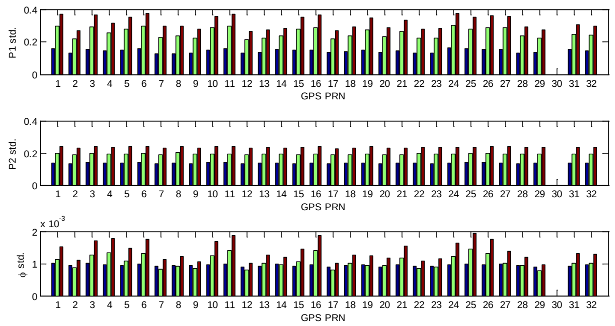

Figure 5: Comparison of STDs for all GPS satellite signals estimated from zero-baseline method (blue bar), time-difference method (green bar) and polynomial prediction method (red bar).

4.2 Case 2: Low sampling rate

To understand the dependency of the proposed methods on the sampling interval, we examine the case with low sampling rate data, e.g. 30 seconds interval data. The data interval is often employed in static GNSS data processing. The description of the test data is given in Table 1. In the short-baseline data processing, the coordinates of the antennas are fixed and the ambiguities are fixed to correct integers. The observation variance is estimated with posterior residuals using the moving window procedure. Three pairs of receivers are tested under the same observation condition. The differences between the estimated observation STD are shown in Figure 6, Figure 7 and Figure 8. Negative value means that the double difference method gives a smaller STD value. The figures shows the estimated observation noise agrees well in high elevation angle case. For elevation angle lower than 20 degree case, the observation STD estimated with the time-difference method and the polynomial prediction method are larger than these from the double difference method. A possible reason is that the amplitude of the ionosphere delay variations is higher in the low elevation case, and the ionosphere delay variation cannot be fully handled by the time-difference method and the polynomial prediction method over 30 seconds interval case. The comparison results also show the STD difference depends on the receiver type and frequency. The carrier phase variance estimated with proposed method is much better than the code variance. The observation variances estimated with the time-difference method and the polynomial prediction method are in 30 sampling rate data case.

Table 1: Test Data description

Description Item	Value
Observation Length	24 hours
Observation Interval	30 second
Observation Date	01/Jan/2014
Receiver Type	Trimble Net R9

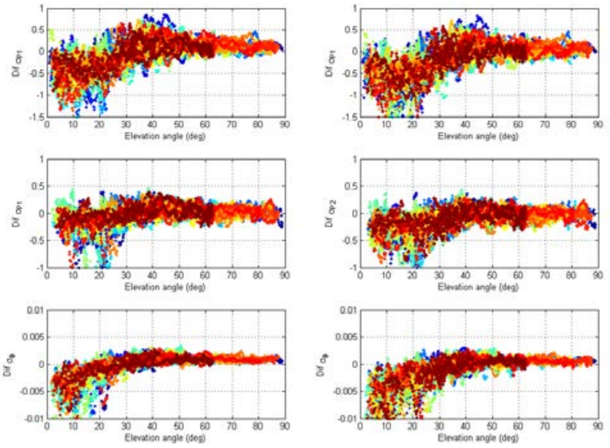

Figure 6: The STD differences between the time-difference method (left column), polynomial prediction method (right column) against the double difference method using Trimble Net R9 receiver. The three rows shows the STD of P1 (upper), P2(middle) and ϕ (lower) respectively.

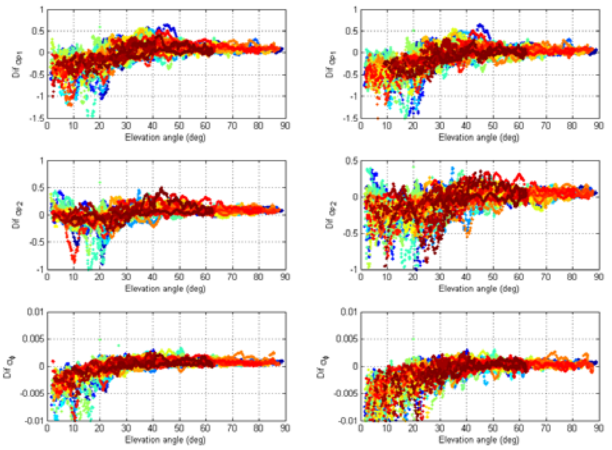

Figure 7: The STD differences between the time-difference method (left column), polynomial prediction method (right column) against the double difference method using Septentrio PolaRX receiver. The three

rows show the standard deviation of P1 (upper), P2(middle) and ϕ (lower) respectively.

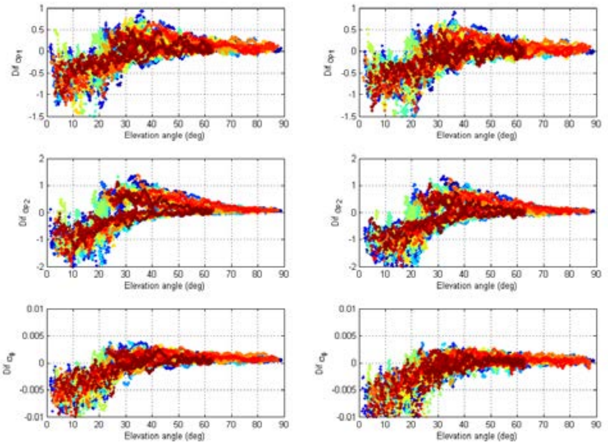

Figure 8: The STD differences between the time-difference method (left column), polynomial prediction method (right column) against the double difference method using Javad TRE_G3 receiver. The three rows shows the standard deviation of P1 (upper), P2(middle) and ϕ (lower) respectively.

5. Impacts of Stochastic Models on Positioning Precision

Ultimately, the performance of the stochastic model should be verified through the positioning results. A good stochastic model should not only improve the positioning results, but also give a more realistic positioning accuracy indicator. The positioning accuracy is usually indicated by the nominal positioning precision calculated from least-squares estimation. However, the nominal precision may not always reflect the real precision properly, partially due to the stochastic model. As a result, the quality control and precision evaluation become uncertain in this case.

With the variance estimated with the observations instead of an empirical value, the estimated nominal precision is expected to be more realistic thus improving the precision evaluation. Figure 9 shows code-based double difference positioning results with empirical observation noise model ($\sigma_P = 0.3m$) and real time estimation methods discussed in section 2. The empirical confidence ellipse/level is estimated by comparing positioning solutions with corresponding true coordinates. Hence, the empirical confidence ellipse/level can be considered as the 'true precision'. The formal confidence ellipse/level is referred to as the nominal precision estimated from least-squares covariance matrix. Normally, the 'true precision' is unknown and the formal one is used as the precision indicator. The figure shows the positioning error with three different stochastic models and their formal and empirical precision. The upper panels show the precision indicator with the constant $\sigma_P = 0.3m$ is too optimistic to reflect the real positioning precision. Both time-differenced method and polynomial prediction method can give more realistic precision indicator. The polynomial prediction method outperforms the time-difference method in this case.

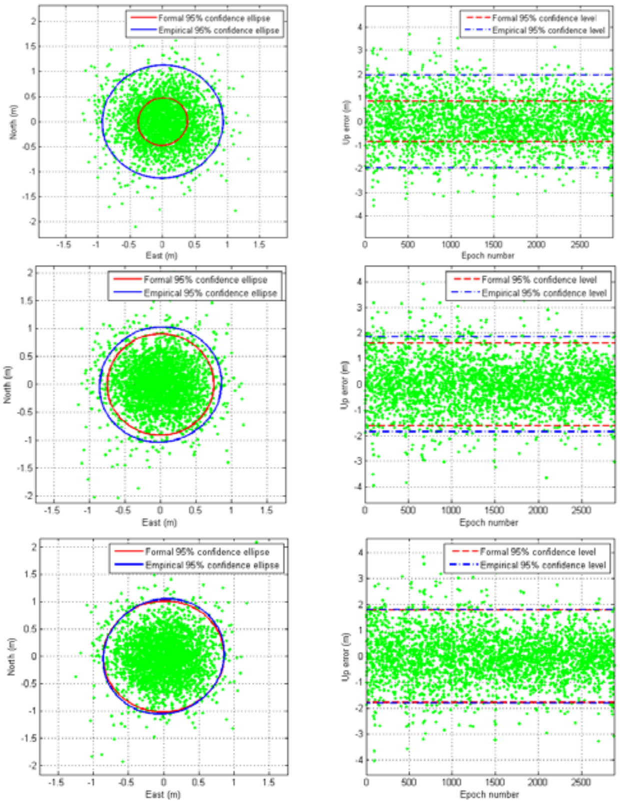

Figure 9: Comparison of the nominal precision with empirical observation noise (upper panels), time-difference method (middle panels) and polynomial prediction method.

The empirical precision with the three stochastic models are listed in Table 2. The table shows that both time-difference method and polynomial prediction method can improve the positioning precision, although the improvement is not as significant as the precision indicator. The time-difference method has comparable positioning performance with the polynomial prediction method.

Table 2: Positioning precision comparison with different stochastic model

Methods	**Std. (E)**	**Std. (N)**	**Std. (U)**
Empirical value $\sigma_P = 0.3m$	0.3829	0.4614	0.9762
Time-difference method	0.3519	0.4231	0.9214
Polynomial prediction method	0.3535	0.4329	0.9125

6. Concluding Remarks

A single receiver based variance estimation method for GNSS data has been developed in this paper. The method can estimate code and phase observation noise with code-phase combination and phase-phase GF combinations respectively. The remaining ionosphere and ambiguity terms are removed by time-difference method or polynomial prediction procedures. The proposed method allows the stochastic model to be estimated in any positioning mode (zero difference/ double difference) and without knowledge of user dynamics (static/kinematic). Another advantage of the proposed method is the independence of the processing on the choices of a position estimator. For instance, the method is suitable for least-squares estimation and Kalman filtering. However, the method may be subject to slow and smooth ionosphere variation and low autocorrelation assumption.

The observation variances estimated with proposed methods are compared with the existing double-difference method. The results show the method agrees the double difference method well in the 1 second case. For the 30 seconds interval case, the proposed method agrees with double-difference method in high elevation segment and could be more conservative in low elevation case. The conservative results may be caused by the ionosphere variations. The impact of the stochastic model on positioning solutions and precision evaluation is also investigated. The results have shown that the proposed method can improve positioning precision and give a more realistic precision indicator.

References

Amiri-Simkooei AR, Tiberius C. (2007). Assessing receiver noise using GPS short baseline time series. GPS solutions, 11, 21-35.

Bona P. (2000). Precision, cross correlation, and time correlation of GPS phase and code observations. GPS solutions, 4, 3-13.

Borre K, Tiberius C. (2000). Time series analysis of GPS observables. In: Proceedings of The 13th International Technical Meeting of the Satellite Division of the Institute of Navigation GPS 2000.

Brunner FK, Hartinger H, Troyer L. (1999). GPS signal diffraction modelling: the stochastic SIGMA-Δ model. Journal of Geodesy, 73, 259-267.

de Bakker PF, Tiberius C, van der Marel H, van Bree RJ. (2012). Short and zero baseline analysis of GPS L1 C/A, L5Q, GIOVE E1B, and E5aQ signals. GPS solutions, 16, 53-64.

de Bakker PF, van der Marel H, Tiberius C. (2009). Geometry-free undifferenced, single and double differenced analysis of single frequency GPS, EGNOS and GIOVE-A/B measurements. GPS solutions, 13, 305-314.

Eueler HJ, Goad CC. (1991). On optimal filtering of GPS dual frequency observations without using orbit information. Journal of Geodesy, 65, 130-143.

Hartinger H, Brunner F. (1999). Variances of GPS Phase Observations: The SIGMA-ε Model. GPS solutions, 2, 35-43.

Jin XX, De Jong CD. (1996). Relationship between satellite elevation and precision of GPS code observations. Journal of Navigation, 49, 253-265.

Kim D, Langley RB. (2001). Estimation of the stochastic model for long-baseline kinematic GPS applications. In: Proceedings of The Institute of Navigation 2001 National Technical Meeting, pp. 586-595.

Langley RB. (1996). Propagation of the GPS signals. In: GPS for Geodesy. Springer, pp. 103-140.

Li B, Shen Y, Xu P. (2008). Assessment of stochastic models for GPS measurements with different types of receivers. Chinese Science Bulletin, 53, 3219-3225.

Tiberius C, Jonkman N, Kenselaar F. (1999). The stochastics of GPS observables. GPS World, 10, 49-54.

Tiberius C, Kenselaar F. (2000). Estimation of the stochastic model for GPS code and phase observables. Survey Review, 35, 441-454.

Tiberius C, Van Der Marel H, Sleewaegen J-M, Boon F. (2008). Galileo down to a millimeter: analyzing the GIOVE-A/B double difference. Inside GNSS, 3, 40-44.

Tiberius CCJM, Van Der Marel H, Sleewaegen J-M, Boon F. (2008). Galileo down to a millimeter: analyzing the GIOVE-A/B double difference. Inside GNSS, 3, 40-44.

Wang J, Satirapod C, Rizos C. (2002). Stochastic assessment of GPS carrier phase measurements for precise static relative positioning. Journal of Geodesy, 76, 95-104.

Biography of Corresponding Author

Lei Wang is a Ph.D candidate in Queensland University of Technology. He received bachelor degree from Wuhan University in 2009. His research interest includes GNSS ambiguity estimation and validation theory and GNSS precise positioning. Email: l62.wang@qut.edu.au